Engineering and Applied Science Letters

PSR Press

Article

Production and characterization of fire-resistant phase change materials for simultaneous thermal energy storage and fire protection in building applications

O. Eyide[1,*], A. Ngbeneme[2], M. H. Ahmed[3], J. I. Ozuligbo[4] and C. S. Onyima[5]

1 Department of Chemical Engineering, University of Delta, Agbor, Delta State, Nigeria
2 Department of Mechanical Engineering, University of Delta, Agbor, Delta State, Nigeria
3 Department of Chemistry, Auchi Polytechnic, Auchi, Edo State, Nigeria
4 Department of Civil and Water Resources Engineering, University of Delta, Agbor, Delta State, Nigeria
5 Alpha Research Laboratory, Awka, Anambra State, Nigeria
* Correspondence: odeworitse.eyide@unidel.edu.ng

Received: 18 February 2026; Accepted: 05 June 2026; Published: 22 June 2026.

Abstract: An FR-PCM composite was produced for the development of an efficient material for thermal energy storage and fire protection through the incorporation of paraffin wax into a cassava starch-oil palm empty fruit bunch lignin-nano-bentonite-boric acid-based biopolymer-mineral matrix. Characterization of the material was done through FTIR, TGA/DTG, scanning electron microscopy (SEM), energy-dispersive spectroscopy (EDS), XRD, Brunauer–Emmett–Teller (BET) analysis, leakage test, thermal cycling, cone calorimetry, smoke-toxicity screening, mechanical properties assessment, and water uptake analysis. FTIR analysis revealed the presence of the C–H bands associated with paraffin wax as well as hydrogen bonding and borate interactions within the biopolymer-mineral matrix. TGA/DTG revealed the increase in the onset of decomposition from about 180 °C for pure paraffin to about 245 °C and the increase in residue at 600 °C from about 15% for pure paraffin to about 30%. Cone-calorimetry smoke/toxicity screening test demonstrated the enhancement in fire performance attributes, such as the increase in time to ignition from 35 s for pure paraffin to 85 s, decrease in peak heat release rate from 900 to 380 kW m^{-2} and decrease in fire growth index from 2600 to 900 W s^{-1}. Laboratory flame-spread testing revealed reduction in flame spread rate from 3.50 to 1.36 cm min^{-1} and increase in ignition delay to 97 s. SEM, EDS, XRD and BET analysis revealed the successful incorporation of biopolymer and mineral materials, maintenance of paraffin crystalline nature, control of mesoporosity and formation of cohesive protective char layer. Leakage and thermal cycling revealed the ability of the matrix to preserve 92% shape retention at 70 °C and more than 90% latent heat retention after 100 thermal cycles. Mechanical and water-uptake properties assessment revealed improvement in the material structural characteristics together with introduction of mild moisture sensitivity. Overall, the FR-PCM composite provides a practical balance between latent heat storage, thermal transport, shape stability, and fire safety for energy-efficient building applications.

Keywords: phase change material, fire resistance, thermal energy storage, paraffin wax, biopolymer composite, bentonite, lignin, building materials

1. Introduction

Buildings require materials with properties to control indoor temperature and minimize fire hazards. Phase change materials (PCMs) are extensively studied in building thermal energy storage since they can absorb and release energy during melting and solidification and thereby enhance the thermal inertia of envelopes, panels, and building systems [1–3]. Paraffin wax is an extensively utilized organic PCM due to its high latent heat capacity, well-reproducible phase change behavior, chemical stability, low tendency to supercool, and proper melting temperatures for passive and active building application [4,5]. Direct utilization of paraffin in buildings is restricted by low thermal conductivity and high flammability [6]. This restriction is crucial in building envelopes, interior panels, insulation boards, and industrial thermal management systems due to the requirement to achieve efficient heat transfer and minimize the fire hazard at the same time [7].

Different techniques such as microencapsulation, shape stabilization, inorganic fillers and addition of flame-retardant additives have been developed in order to minimize the leakage, enhance the thermal transport and fire behavior of organic PCMs [8–11]. Most of the published results are concerned with petroleum-based polymeric shells, synthetic flame retardants or expensive hybrid fillers which may increase the cost and decrease the environmental compatibility of systems [12,13]. Therefore, environmentally-friendly alternatives based on natural binders and abundant mineral fillers should be developed for affordable construction and industrial facilities in cases when local raw materials can ensure their production [14,15]. In this regard, an appropriate PCM should have latent heat storage properties and also delay ignition, suppress flame spread and preserve the integrity after exposure to fire.

In this respect, cassava starch, oil-palm empty fruit bunch (OPEFB) lignin, bentonite clay and boric acid could provide complementary features. Cassava starch is capable of forming a continuous matrix after gelatinization, lignin provides aromatic char-forming structure, nano-bentonite is a thermally stable layered filler and boric acid can react with hydroxyl groups of biopolymers to promote dehydration and char formation [16–19]. All these components are applicable in the concept of the material design, when paraffin provides latent heat storage and surrounding matrix provides fire resistance, leakage suppression and mechanical stability.

The research question of this work is if it is possible to create a cheap biopolymer-mineral matrix, which would transform highly flammable paraffin wax into FR-PCM possessing both thermal energy storage and fire performance improvement. The originality of the approach is in combination of cassava starch, OPEFB lignin, nano-bentonite, boric acid, glycerol and paraffin into one composite system providing latent heat storage, enhancement of the thermal conductivity, char formation, suppression of the leakage and post-fire structural stability. This balance is evaluated using different chemical, thermal, morphological, structural, porosity, fire and smoke resistance, mechanical and moisture response properties.

2. Materials and Methods

2.1. Materials

The cassava starch was purchased from local food-processing centers in Boji Boji Owa, Agbor, Delta State, Nigeria. Lignin was isolated from OPEFB which is agro-industrial residue obtained from Owa-Alero, Agbor, Delta State, Nigeria. Raw bentonite clay was obtained from Anambra State, Nigeria and was purified prior to modification to the nano-scale. Paraffin wax was acquired from Owa-Oyibo Market, Agbor, Delta State, Nigeria. The distilled water, boric acid, and glycerol were all obtained from Alpha Research Laboratory, Awka, Anambra State, Nigeria.

2.2. Lignin extraction and nano-bentonite preparation

Lignin was isolated from OPEFB using the alkaline pulping process. OPEFB fibers (50 g) were incubated in 10% (w/v) sodium hydroxide aqueous solution at 90 °C for 1 hour while subjected to mechanical stirring. The solid residue was separated from black liquor containing the lignin through filtration. The black liquor was further acidified to pH 2.0 using concentrated hydrochloric acid for the precipitation of the lignin. The precipitated lignin was recovered through filtration, washed with distilled water to rinse out any remaining alkali or other impurities, oven-dried to constant weight at 60 °C and stored in sealed vessels.

The raw bentonite was dispersed in distilled water in a ratio of 1:10 (w/v). The dispersion was oxidized with 1% (v/v) hydrogen peroxide to eliminate organic contaminants. The oxidation product was then centrifuged and dried. Particle size reduction was carried out with high-energy planetary ball mill (Retsch PM 100) for 2 hours. The milled product was then acid activated using 0.5 M hydrochloric acid to improve its surface characteristics and increase its dispersion properties.

2.3. Preparation of the FR-PCM composite

Cassava starch was dispersed in distilled water and heated to 80 °C to gelatinize while constantly stirred mechanically to obtain the homogeneous viscous matrix. Lignin and nano-bentonite were introduced into the starch matrix under agitation at 500 rpm. In another vessel, paraffin wax was melted at 70 °C and then mixed with the biopolymer-mineral matrix under continuous stirring. Boric acid was incorporated as

a flame-retardant crosslinking agent and glycerol to improve the flexibility and toughness of the composite. The final mixture was homogenized and poured into molds and dried at 60 °C for 24 hours.

All formulations were calculated in a relative weight percentage basis, except distilled water that was only used as processing media. The optimized formulation had 78.9 wt% paraffin wax, 10 wt% cassava starch, 5 wt% OPEFB lignin, 3 wt% nano-bentonite, 2 wt% boric acid, and 2 wt% glycerol. Table 1 shows that the pure PCM served as energy storage baseline, the FR-PCM composite was the multifunctional system while the blank matrix was the fire retardant matrix without paraffin.

Table 1. Experimental formulation matrix for the PCM systems

Sample	Paraffin wax	Cassava starch	OPEFB lignin	Nano-bentonite	Boric acid	Glycerol
Pure PCM	100 wt%	–	–	–	–	–
FR-PCM composite	78.9 wt%	10 wt%	5 wt%	3 wt%	2 wt%	2 wt%
Blank matrix	–	57.0 wt%	19.0 wt%	9.5 wt%	9.5 wt%	5.0 wt%

2.4. Characterization of chemistry, structure, and morphology

FR-PCM composite materials were analyzed for chemical reactions, morphology, thermal properties, thermal conductivity, phase change properties, and flame resistance performance. The FTIR spectra were recorded in the range of 4000 to 400 cm^{-1} using Shimadzu IRTracer-100 spectrophotometer. Paraffin C–H stretching vibration bands, starch and lignin hydroxyl groups, aromatic lignin functional groups, borate bonding, and bentonite Si–O–Si bending vibrational bands were analyzed.

SEM was used to study surface morphology, fractured morphology, dispersion of filler material, confinement of paraffin wax, and morphologies of post combustion char products at accelerating voltage of 15 kV. Bentenote nanoparticles were studied by using SEM, TEM, DLS, and XRD techniques to confirm platelet shape structure, nanoscale dispersion, and crystalline structure of montmorillonite in acid activated bentonite.

2.5. Differential scanning calorimetry

Differential scanning calorimetry (DSC) was done in the range of 20 to 100 °C at heating rate of 10 °C min^{-1} under nitrogen atmosphere. The melting temperature was calculated from endothermic peak and latent heat of fusion was calculated from integration of endothermic peak. The latent heat retention was calculated by Eq. (1):

$$\eta_L = \left(\frac{\Delta H_{m,\text{FR-PCM}}}{\Delta H_{m,\text{PCM}}} \right) \times 100, \tag{1}$$

where η_L is latent heat retention (%), $\Delta H_{m,\text{FR-PCM}}$ is the latent heat of fusion of the FR-PCM composite (J g^{-1}), and $\Delta H_{m,\text{PCM}}$ is the latent heat of fusion of pure paraffin PCM (J g^{-1}).

2.6. Thermogravimetric analysis

Thermogravimetric analysis was conducted from 25 to 600 °C at 10 °C min^{-1} under nitrogen flowing at 50 mL min^{-1}. Onset degradation temperature, $T_{5\%}$, maximum degradation temperature, and residual char yield were determined. The percentage improvement in onset degradation temperature was calculated from Eq. (2):

$$I_T = \left(\frac{T_{\text{onset,FR-PCM}} - T_{\text{onset,PCM}}}{T_{\text{onset,PCM}}} \right) \times 100, \tag{2}$$

where I_T is thermal stability enhancement (%), $T_{\text{onset,FR-PCM}}$ is the onset degradation temperature of the composite, and $T_{\text{onset,PCM}}$ is the onset degradation temperature of neat paraffin.

2.7. Thermal conductivity measurement

Effective thermal conductivity was determined by the steady-state guarded hot-plate/Lee's disc method. Layers of the composite of identical thicknesses (0.5 ± 0.05 mm) were deposited on mild steel plates of dimensions 100 mm × 100 mm. Guard heaters were used to ensure that both surfaces of the specimens were in thermal contact. Temperatures were recorded using calibrated thermocouples. Calibration of the system was done using metals of known thermal conductivity. The steady state was taken to have been reached when

fluctuations in heat flux and temperature difference were less than 1% over 30 min. Surfaces were polished, thermal grease was applied in a thin layer, and even clamping was done to minimize contact resistance. The measurements were carried out in triplicate, with results presented as mean ± standard deviation.

The measured response is due to the thermal resistance of the coating, substrate, and contacts. Series thermal resistance can be represented as Eq. (3):

$$R_{\text{tot}} = \frac{L_{\text{coat}}}{k_{\text{coat}}A} + \frac{L_{\text{sub}}}{k_{\text{sub}}A} + R_{\text{contact}}, \tag{3}$$

where R_{tot} is total thermal resistance (K W^{-1}), L_{coat} and L_{sub} are the coating and substrate thicknesses, k_{coat} and k_{sub} are their thermal conductivities, A is cross-sectional area, and R_{contact} is interfacial contact resistance. The incremental resistance introduced by the coating is given by Eq. (4):

$$\Delta R = R_{\text{tot}} - R_{\text{tot,uncoated}} = \frac{L_{\text{coat}}}{k_{\text{coat}}A} + \Delta R_{\text{contact}}. \tag{4}$$

For one-dimensional steady-state heat flow through a homogeneous layer, thermal conductivity was calculated using Eq. (5):

$$k = \frac{qL}{A\Delta T}, \tag{5}$$

where q is heat-flow rate, L is layer thickness, A is cross-sectional area, and ΔT is the temperature difference across the layer. Thermal-conductivity enhancement relative to pure PCM was calculated using Eq. (6):

$$E_k = \left(\frac{k_{\text{FR-PCM}} - k_{\text{PCM}}}{k_{\text{PCM}}}\right) \times 100. \tag{6}$$

2.8. Ignition and Flame-Spread Assessment

A lateral ignition and flame spread method based on ASTM E1321-21 and a screening laboratory test according to ASTM E84 was used to investigate ignition and flame-spread behavior. In this regard, a LIFT test set-up with electrically heated ceramic radiant panel was used to generate incident heat flux from 10 to 60 kW m^{-2}. The surface heat flux was assessed using a water-cooled Schmidt–Boelter gauge with a traceable calibration to a standard at NIST. Premixed methane-air pilot burner with a rectangular slot configuration placed at the lower edge of specimens was used to ignite the samples.

The specimens were arranged vertically in such a way that the coated side faced the radiant panel at a distance of 50 mm. Such arrangement resulted in the generation of heat flux equal to 35 kW m^{-2} at the ignition end and a decreasing heat-flux gradient across the length of the specimen. A calibrated scale divided into 10 mm sections was put next to each specimen for flame-front measurements. Prior to the tests, the radiant panel was stabilized for 10 minutes. Sustained ignition was considered as flame burning for more than 5 seconds. Flame-spread velocity was calculated by Eq. (7):

$$v_{\text{fs}} = \frac{\Delta x}{\Delta t}, \tag{7}$$

where Δx is flame front propagation distance and Δt is propagation time. Data collection was carried out over an approximate center distance of 60 mm to eliminate any edge effect.

Critical heat flux, ignition factor of the material, and flame spread factor were obtained from ignition and spread results. The reduction in flame spread compared with neat PCM was determined from Eq. (8):

$$R_{\text{fs}} = \left(\frac{V_p - V_c}{V_p}\right) \times 100, \tag{8}$$

where V_p is the flame-spread rate of pure PCM and V_c is the flame-spread rate of the FR-PCM composite. The percentage change in any fire-performance parameter was calculated using Eq. (9):

$$\%\Delta = 100 \times \frac{X_{\text{FR-PCM}} - X_{\text{PCM}}}{X_{\text{PCM}}}. \tag{9}$$

All experiments were performed in triplicates ($n = 3$). One-way ANOVA was used at $p < 0.05$. The test was stopped in case of reaching upper edge, self-extinguishing after flames for over 10 s, maximal burning period of 300 s or structural failure. Uniformity of heat flux on the radiant panel was kept within ±5% deviation of heat flux.

2.9. Evaluation of post-burn char quality

The surfaces of burned samples were photographed after the flame-spread test by using digital optical camera placed perpendicular to the specimen and kept constant at 30 cm distant from it with uniform illumination. Scale bar of 10 mm length was provided with each photo. The evaluation of char morphology was done by ImageJ software. Continuity of the chars was calculated as the proportion of continuous area covered with the char. The number of visible cracks per unit area was counted as the crack density (cracks cm^{-2}). The delamination area was defined as a ratio of the area of separated fragments to total char area.

Three independent raters examined randomized photos without knowing the type of samples. Each of them quantitatively evaluated the char morphology and characterized the char integrity as poor, moderate or excellent according to the above described criteria. Inter-rater reliability was estimated by Cohen's kappa coefficient (κ). Its value over 0.80 was considered as strong agreement. Values presented are the means of independent measurements. The final assessment was made in consensus between raters.

2.10. Screening of thermal stability and smoke toxicity

The cone calorimetry screening was performed according to the ISO 5660 / ASTM E1354 standards to measure heat release rate, ignition time, mass loss, residual mass, smoke production and gas emissions in controlled conditions of heating. Screening of smoke and toxicity involved optical attenuation and gas analysis.

3. Results and discussion

3.1. FTIR analysis

As demonstrated by the FTIR spectra of Figure 1, the incorporation of paraffin wax into the bio-based fire-resistant matrix occurred successfully. The spectra of pure PCM revealed intense aliphatic C–H stretching bands near 2920 and 2850 cm^{-1}, typical for hydrocarbons of paraffin. These bands still exist in the spectrum of the FR-PCM composite, proving that paraffin phase remains even after the matrix incorporation. The blank matrix reveals a wide O–H stretching band between 3200 and 3500 cm^{-1} attributed to hydroxyl groups of starch and lignin. In the spectrum of the FR-PCM composite, this band gets broader and shifted, proving the formation of hydrogen bonds between starch, lignin, borate compounds, and hydroxylated surfaces of nano-bentonite.

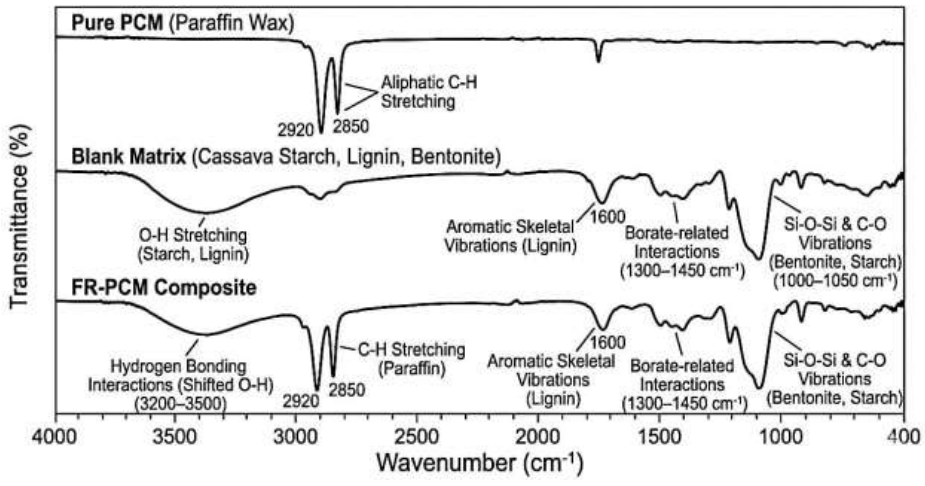

Figure 1. FTIR spectra of pure PCM, blank matrix, and FR-PCM composite

There was a band near 1600 cm^{-1} related to vibrations of aromatic skeleton of lignin and another one at 1300-1450 cm^{-1} related to the borate interactions. The presence of the Si-O-Si and C-O bands between 1000 and 1050 cm^{-1} confirmed the contribution of bentonite and polysaccharides. Coexistence of bands corresponding to paraffin, biopolymer, borate, and bentonite in the FTIR spectra confirms the absence of any destruction of the PCM. Broadening and shifting of the FTIR bands reveal better interfacial interaction of the components and explain char formation, leakage prevention, and increased thermal stability.

3.2. TGA behaviour

Thermogravimetry and derivative thermogravimetry techniques were used for comparison of degradation characteristics, mass losses and char formation ability. The values of TGA parameters presented in Table 2 reveal that pure PCM was the least stable in terms of thermal stability, with onset of degradation around 180 °C, temperature of 5% mass loss around 185 °C and maxima of degradation around 280 °C. This indicates rapid volatilization and thermal decomposition of paraffin wax [20]. Residual mass at temperature 600 °C was around 0–1%, which means paraffin does not produce protective char.

Table 2. TGA/DTG degradation parameters and char-forming performance

Parameter	Pure PCM	FR-PCM composite	Blank matrix
Initial degradation temperature (°C)	180	245	∼130
$T_{5\%}$ (°C)	185	250	∼210
T_{max} (°C)	280	290	∼330
Residual mass at 600 °C (%)	∼0–1	29–30	∼65
Char yield at 600 °C (%)	Trace/not significant	29	∼65
Performance interpretation	Low thermal stability and negligible residue formation	Enhanced thermal stability and effective char formation	Multi-stage degradation with high char/mineral residue and strong thermal reinforcement
Thermal energy storage rating	Very high	High	Low
Fire protection rating in buildings	Poor	High	Very high
General suitability for building TES applications	High latent heat storage but unsafe under fire exposure	Best balance of TES capacity and thermal/fire stability	Excellent thermal shielding and fire resistance but limited TES function

The FR-PCM composite raised the onset temperature of the degradation process to approximately 245 °C, and $T_{5\%}$ value to about 250 °C. The residual amount of the material was 29–30% at 600 °C, which demonstrates good condensed-phase protection. It is possible to say that such features are due to the combination of lignin, starch, boric acid and nano-bentonite. The lignin adds aromatic carbon structures, the boric acid increases dehydration and char stabilization, and the bentonite strengthens the residual layer. The maximum residue in the blank matrix (approximately 65%) is related to the significant presence of char-forming biopolymer and mineral constituents, which are thermally stable, in the composition of the material but do not contain latent heat storage phase.

From the comparison of the curves shown in Figure 2, it is clear how the fire retardant matrix impacts the properties of the FR-PCM composite. The pure paraffin did not change its weight from 25 to 150 °C, then decomposed rapidly from approximately 180 to 350 °C, leaving almost no residue at 600 °C. The curve of DTG contained a sharp peak at 280 °C, which means one decomposition step. For the FR-PCM composite, there was a moisture loss zone at low temperatures, a delay in the main decomposition process near 245 °C, a paraffin-related DTG peak at 290 °C, and wider shoulders in the range of 300–500 °C. It is related to the fact that this material undergoes the multistep decomposition process, first starch, lignin and matrix components decomposition, and then the formation of the char layer.

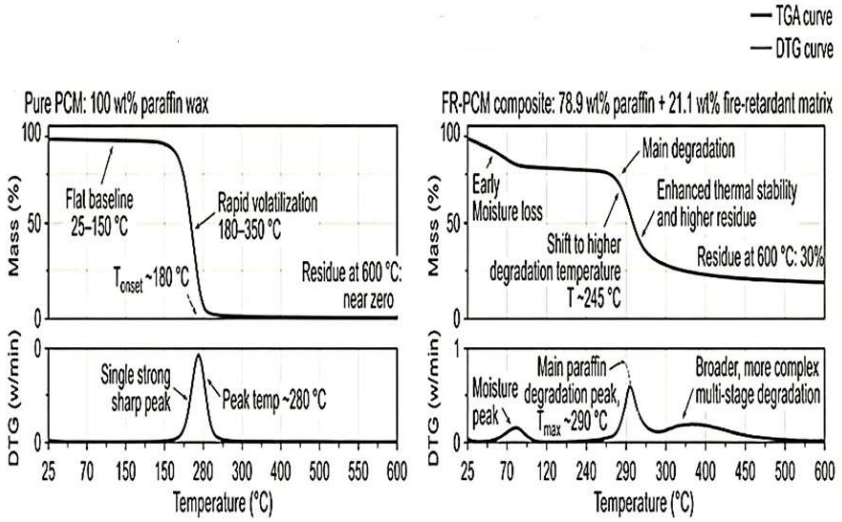

Figure 2. TGA/DTG profiles of pure PCM and FR-PCM composite

From the blank matrix profile presented in Figure 3, the inherent heat resistance of the starch–lignin–bentonite–borate matrix can be seen. Initially, the mass loss before 150 °C is due to absorbed and bound water. The following degradation peak at 260 °C is largely due to starch and glycerol pyrolysis, whereas the broad peak from 300 °C to 500 °C represents the slow process of lignin degradation. The high residue present in this profile indicates that the matrix provides the main mechanism for condensed phase protection of the FR-PCM. Combined, Figures 2 and 3 reveal how the matrix transforms the process of decomposition from fast paraffin volatility to a regulated process of multistage decomposition with significant residual barrier creation.

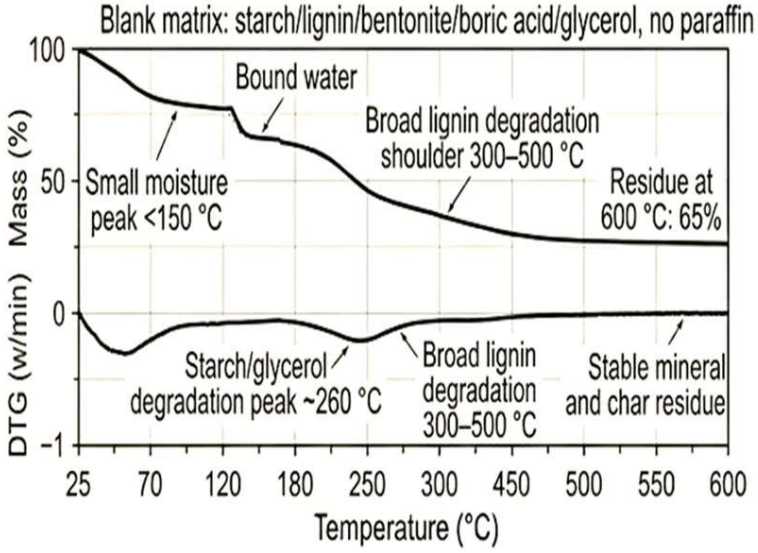

Figure 3. TGA/DTG behavior of the blank fire-retardant matrix

3.3. Laboratory Flame-spread Screening

The flame-spread screening results from Table 3 clearly show the fire performance improvement achieved via the matrix. The pure PCM sample ignited very quickly after 38.0 ± 2.0 seconds and gave a flame-spread rate of 3.50 ± 0.06 cm min^{-1}, which confirms that it is highly flammable and gives low post-fire residues. The FR-PCM composite sample increased ignition time to 97.0 ± 3.6 s while reducing flame spread rate to 1.36 ± 0.04 cm min^{-1}. The residue of this composite sample increased to 29.0 ± 0.4% due to the formation of char which slows down heat conduction and release of volatiles.

Table 3. Laboratory ignition, flame-spread, and residue results

Sample	Ignition time (s, mean ± SD)	Flame-spread rate (cm min^{-1}, mean ± SD)	Residue (%, mean ± SD)
Pure PCM	38.0 ± 2.0	3.50 ± 0.06	2.5 ± 0.3
FR-PCM composite	97.0 ± 3.6	1.36 ± 0.04	29.0 ± 0.4
Blank matrix	121.0 ± 3.0	0.85 ± 0.03	47.5 ± 0.7

The blank matrix sample took the longest time to ignite (121.0 ± 3.0 s), spread flames the slowest (0.85 ± 0.03 cm min^{-1}), and had the greatest screening residue (47.5 ± 0.7%). It indicates superior fire-retardancy owing to the good protective capacity of the starch–lignin–bentonite–borate matrix. But for building TES, the FR-PCM is more appropriate as it offers both fire safety and heat energy storage.

3.4. Fire performance and char integrity

The analysis of fire performance (Table 4) demonstrates that although the pure PCM offers excellent thermal energy storage, it is not fire-safe as it ignites instantly, spreads the flame fast, and leaves char residue with cracks and delaminations. There were considerable improvements in the FR-PCM composite with regard to increased ignition time to 97 s, reduced flame-spreading rate to 1.36 cm min^{-1}, and improved char integrity to high levels. It is due to lignin carbonization, borate dehydration effect, and clay barrier protection. The blank matrix sample was the best in terms of fire protection owing to its dense char–mineral residue, but it did not have paraffin, hence poor TES rating.

Table 4. Fire performance, char integrity, and TES suitability

Parameter	Pure PCM	FR-PCM composite	Blank matrix
Ignition delay (s)	38	97	121
Flame-spread rate (cm min^{-1})	3.50	1.36	0.85
Char continuity (%)	Low reference baseline	High; continuous compact char layer	Very high; dense char–mineral network
Crack density (cracks cm^{-2})	High qualitative reference	Low	Very low
Delamination area (%)	High reference baseline	Low	Minimal
Spallation mass loss (%)	High reference baseline	Significantly reduced	Very low
Char integrity level	Poor	High	Very high
Thermal energy storage rating	Very high	High	Low
Fire protection rating in buildings	Poor	High	Very high
Overall suitability for building TES applications	Limited by high flammability	Best overall balance of TES and fire safety	Excellent fire barrier but limited TES capability

As can be seen from the rating criteria in Table 5, the pure PCM is in the lowest category, the FR-PCM in a high-performance category for multifunctional TES application, while the blank matrix in the strongest fire barrier category. This difference is significant since, along with being able to withstand flames, the target material has to provide latent heat accumulation and its release. Thus, the FR-PCM is a most useful balance between fire resistance, TES and post-flame performance [21].

Table 5. Rating criteria for fire-performance evaluation

Rating	Level	Quantitative criteria	Qualitative description	Interpretation
Fail	Very low	Ignition delay < 60 s and flame-spread rate > 3 cm min^{-1} with poor char integrity	Immediate ignition and no effective protective char	Poor fire resistance with rapid flame propagation and inadequate thermal shielding
Pass	Low	Ignition delay ≥ 60 s and flame-spread rate ≤ 2.5 cm min^{-1} with moderate char integrity	Limited resistance to flame spread and discontinuous char	Weak thermal-barrier effect with limited fire protection
Good	Moderate	Ignition delay ≥ 100 s and flame-spread rate ≤ 1.5 cm min^{-1} with excellent char integrity	Delayed ignition with compact and relatively stable char	Acceptable fire-retardant performance with moderate insulation and structural stability
Best	High/very high	Ignition delay ≥ 120 s and flame-spread rate ≤ 1.0 cm min^{-1} with excellent char integrity and minimal delamination	Significant ignition delay with dense continuous char and suppressed flame spread	Excellent fire-retardant performance with strong thermal-barrier action

3.5. Thermal conductivity improvements

From the values obtained for thermal conductivity shown in Table 6, it is evident that the pure PCM had the lowest value of 0.24 W m^{-1} K^{-1}; this is characteristic of paraffin wax and inhibits the heat charging/discharging process. By adding the FR-PCM composite, the conductivity was improved to 0.31 W m^{-1} K^{-1}, which translates to an improvement of around 28-29%. This increase indicates that the nano-bentonite, lignin, starch, and borate-containing matrix created more efficient solid heat-transfer pathways while preserving latent heat functionality.

Table 6. Thermal conductivity, energy storage, and fire-safety performance

Parameter	Pure PCM	FR-PCM composite	Blank matrix
Thermal conductivity (W m^{-1} K^{-1})	0.24	0.31	~0.36–0.40
Thermal-conductivity change	Reference	Approximately 28–29% increase	Higher than FR-PCM due to mineral-rich structure
Interpretation	Low heat-transfer rate typical of paraffin wax	Improved heat-transfer efficiency through filler-supported pathways	Enhanced conduction from dense lignin–mineral network
Thermal energy storage rating	Very high	High	Low
Fire protection rating in buildings	Poor	High	Very high
Overall suitability for building TES applications	Excellent latent heat storage but limited by low conductivity and flammability	Best balance of thermal conductivity, TES, and fire safety	Excellent thermal/fire barrier but limited latent heat storage

The blank matrix possessed the highest thermal conductivity, approximately 0.36–0.40 W m^{-1} K^{-1}, due to its highly conductive mineral-carbonaceous structure. However, the absence of paraffin makes this high thermal conductivity unusable for latent heat storage. Thus, the FR-PCM is the optimal material for building TES as it enhances the heat transfer process without loss of the phase change properties, while also providing enhanced fire resistance.

3.6. SEM morphology before and after burning

As it can be seen from SEM images presented in Figure 4, there are visible differences in morphologies of studied materials before and after burning. Pure PCM had a relatively smooth and wax-like surface before burning, which indicates its solid paraffin structure. FR-PCM composite had a heterogeneous surface with paraffin regions, dispersed particles and micro-pores, thus proving that the matrix and the fillers were added in the PCM phase. Blank matrix was characterized by a rough and porous surface, corresponding to the structure of the starch-lignin-clay network.

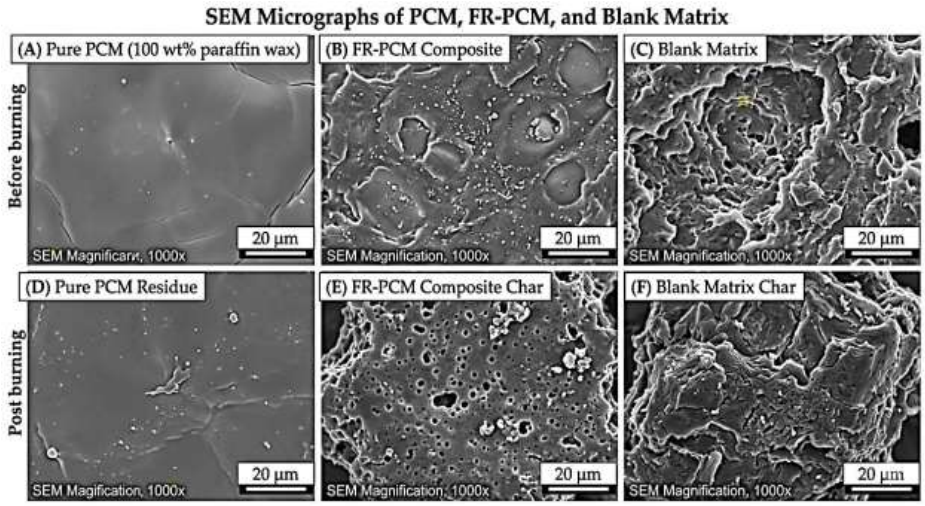

Figure 4. SEM micrographs of pure PCM, FR-PCM composite, and blank matrix before and after burning

After burning, only some remnants of pure PCM could be observed, proving its low capability of charring. FR-PCM composite formed a porous, yet continuous layer of char with mineral particles embedded in it. It

is important as pores and mineral particles help dissipate heat, release volatiles slowly and provide cohesive char during burning. Blank matrix formed the densest char/mineral layer, as was confirmed by higher residual mass. The results presented in Table 7 are consistent with the results of TGA and flame-spread tests and prove the char-forming effect of the matrix.

Table 7. SEM morphological observations

Sample condition	Observed morphology	Interpretation
Pure PCM before burning	Smooth wax-like surface with limited visible porosity	Typical solidified paraffin morphology
FR-PCM before burning	Heterogeneous surface with paraffin-rich domains and dispersed matrix/filler features	Paraffin retained within a fire-retardant matrix
Blank matrix before burning	Rough porous biopolymer–clay network	Formation of non-PCM fire-retardant matrix
Pure PCM residue	Minimal smooth residue after burning	Poor char-forming ability of pure paraffin
FR-PCM char	Porous char with embedded particles	Condensed-phase barrier formation during burning
Blank matrix char	Dense rough char/mineral residue	High residue from matrix constituents

3.7. EDS and XRD analysis

The EDS and XRD data confirm that the fire-retardant inorganic additives were added to the FR-PCM matrix, while maintaining the crystallinity of paraffin. In Fig. 5, the EDS analysis of pure PCM reveals a carbon-based structure and distinct diffraction lines at about 21.6° and 23.9° 2θ due to paraffin crystallites in XRD pattern, which confirms the presence of crystalline hydrocarbons in PCM. The EDS spectrum of the FR-PCM composite also had high carbon content along with the oxygen, silicon, aluminum, and minor boron content due to the incorporation of starch, lignin, bentonite, and boric acid. The XRD pattern of FR-PCM still contained paraffin diffraction lines and hence, confirms that the matrix did not damage the PCM crystallites, which are essential for latent heat storage.

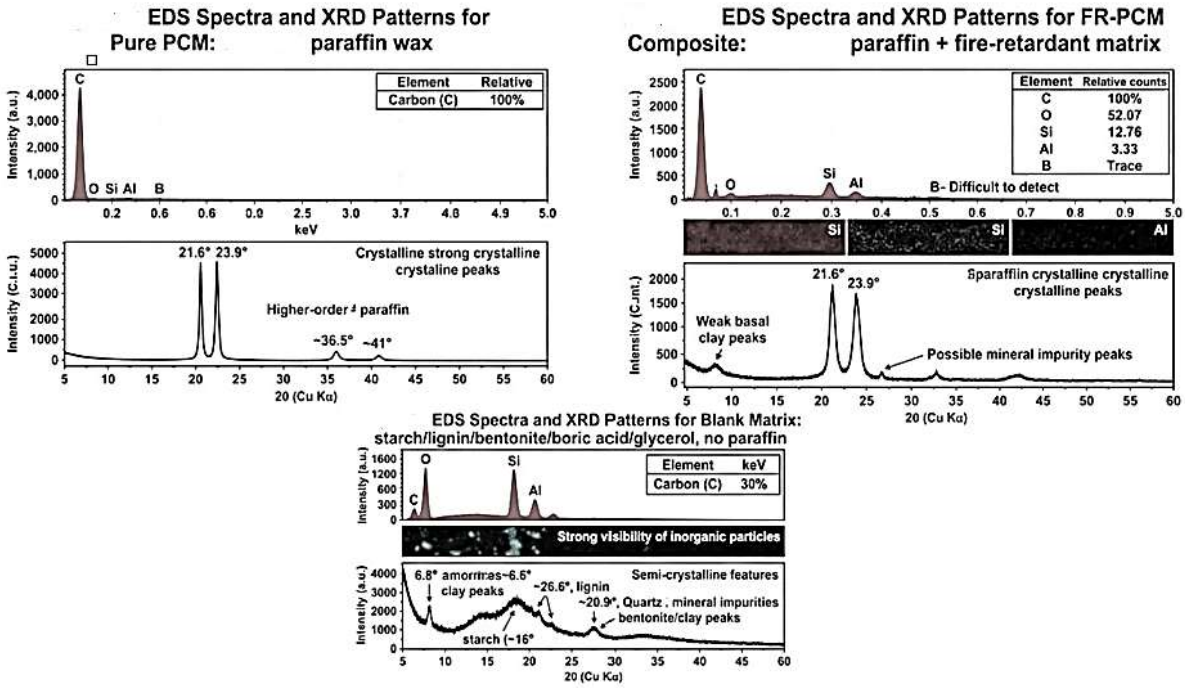

Figure 5. EDS spectra and XRD patterns of pure PCM, FR-PCM composite, and blank matrix

The blank matrix possessed more pronounced inorganic chemical properties and semicrystalline structures linked to starch, lignin, clay, borate, and minerals. Table 8 highlights the structural contrasts. The critical insight gained from this analysis is that the FR-PCM possesses the two important structural properties required: preserved paraffin crystals for heat storage and inorganic/biopolymer material for fire-resistance.

Table 8. EDS and XRD features with structural interpretation

Sample	EDS features	XRD features	Interpretation
Pure PCM	Carbon-dominant spectrum; no strong Si/Al/B peaks	Strong paraffin peaks at 21.6° and 23.9° 2θ; weak higher-order paraffin peaks	Pure hydrocarbon wax with high paraffin crystallinity
FR-PCM composite	C dominant; O, Si, and Al present; B trace/difficult to detect	Paraffin peaks retained; weak clay/mineral reflections present	Paraffin crystallinity preserved while matrix/filler components are incorporated
Blank matrix	C, O, Si, and Al visible; stronger inorganic contribution	Clay peaks at low 2θ, starch feature near 16°, lignin/amorphous band near 20.9°, and quartz/mineral peak near 26.6°	Biopolymer–clay–borate matrix without paraffin-dominant crystallinity

3.8. BET surface area and porosity

The nitrogen adsorption-desorption BET behavior shown in Figure 6 and Table 9 clearly shows the effect of paraffin filling on the pores of the matrix. Pure paraffin showed minimal nitrogen adsorption, BET surface area less than 1 m^2 g^{-1} and pore volume less than 0.005 cm^3 g^{-1}, which confirms the presence of dense non-porous wax phase. Blank matrix had the maximum surface area (85 m^2 g^{-1}), pore volume (0.18 cm^3 g^{-1}) and mesopore size of around 10 nm, showing the porous nature of starch-lignin-bentonite-borate composite.

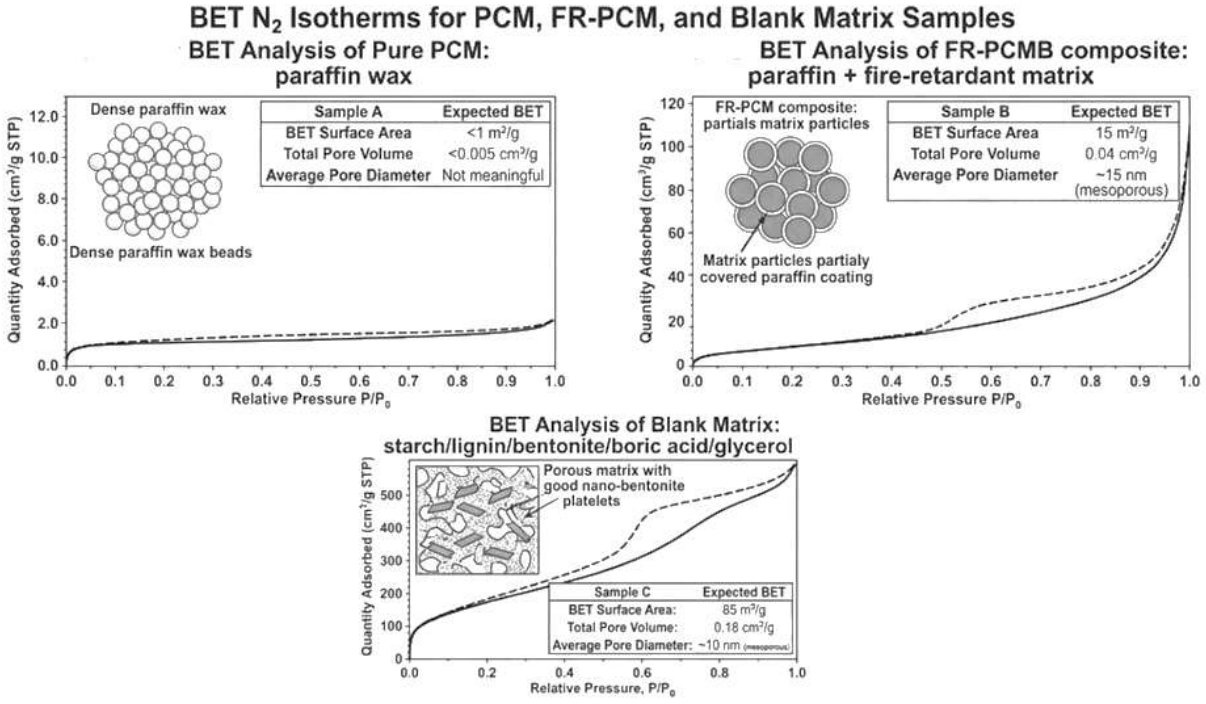

Figure 6. BET nitrogen adsorption/desorption isotherms and surface-area parameters

Table 9. BET surface area and pore-structure characteristics

Parameter	Pure PCM	FR-PCM composite	Blank matrix
BET surface area (m^2 g^{-1})	< 1	15	85
Total pore volume (cm^3 g^{-1})	< 0.005	0.04	0.18
Average pore diameter	Not meaningful	~15 nm	~10 nm
Interpretation	Dense nonporous paraffin wax	Intermediate mesoporous structure; matrix pores partially filled/coated by paraffin	Porous starch, lignin, bentonite, and borate matrix
Thermal energy storage rating	Very high	High	Low
Fire protection rating in buildings	Poor	High	Very high
Overall suitability for building TES applications	Excellent latent heat storage but structurally unstable without support	Best balance of PCM confinement, thermal performance, and fire safety	Excellent fire-resistant scaffold but limited TES capability

The composite FR-PCM had intermediate textural characteristics: the BET surface area was equal to 15 m^2 g^{-1}, pore volume was 0.04 cm^3 g^{-1}, and mean diameter of pores – 15 nm. Reduction of surface area and pore volume in comparison with the blank matrix implies partial filling of pores with paraffin, which is useful since it ensures PCM immobilization during melting, increases the contact area of PCM with matrix, and contributes

to char formation during heating up in flames. Thus, FR-PCM takes advantage from pores in the matrix, using them not as cavities but as confined spaces.

3.9. Leakage resistance and thermal-cycling stability

The leakage test performed at temperature 70 °C for 2 hours (Table 10) demonstrates the effect of matrix confinement on leakage. Pure PCM melted completely, was distributed over the area of 35 ± 4 cm^2, was lost by 92 ± 5 wt%, and its form retention was equal to 5 ± 3%. It means that free paraffin cannot be applied directly in buildings except for being enclosed. The composite FR-PCM reduced the leakage area to 4.5 ± 1.0 cm^2, mass loss to 4.8 ± 1.1 wt%, and form retention increased to 92 ± 4%. The blank matrix showed no melting and almost complete shape stability, but it did not provide latent heat storage.

Table 10. Leakage-testing results at 70 °C for 2 h

Parameter	Pure PCM	FR-PCM composite	Blank matrix
Initial mass (g)	10.00 ± 0.02	10.00 ± 0.02	10.00 ± 0.02
Visible melting	Complete melting	Softening/limited surface wax possible	No melting
Visible leakage area (cm^2)	35 ± 4	4.5 ± 1.0	0
Leakage mass loss (wt%)	92 ± 5	4.8 ± 1.1	0.3 ± 0.2
Shape retention after test (%)	5 ± 3	92 ± 4	98 ± 1
Post-test appearance	Collapsed wax pool	Mostly intact; slight edge staining	Intact dry matrix

After 100 thermal cycles of temperature variation from 20 to 70 °C, it was found that FR-PCM possessed consistent phase transition behavior (Table 11). The difference in the melting temperature of FR-PCM was only 52.0 ± 1.5 °C to 51.2 ± 1.7 °C while latent heat retention capacity was 91.5 ± 3.5%. The latent heat retention of pure PCM was higher if it was kept sealed. But if it was not sealed, there were chances of leakage of the material.

Table 11. Thermal-cycling stability over 100 cycles between 20 and 70 °C

Parameter	Pure PCM	FR-PCM composite	Blank matrix
Cycle count	100	100	100
Mass loss after cycling (wt%)	1.2 ± 0.4 if sealed; high if unsealed	2.8 ± 0.8	1.8 ± 0.6
Melting peak before cycling (°C)	52.0 ± 1.0	52.0 ± 1.5	No PCM peak
Melting peak after cycling (°C)	51.5 ± 1.2	51.2 ± 1.7	No PCM peak
Initial latent heat (J g^{-1})	180 ± 5	142 ± 4	Not applicable
Latent heat after cycling (J g^{-1})	174 ± 6	130 ± 5	Not applicable
Latent heat retention (%)	96.7 ± 3.0	91.5 ± 3.5	Not applicable
Visual leakage after cycling	Possible if unsealed	Low/slight edge staining	None

3.10. Conical calorimetry and screening for smoke and toxicity

The results obtained during cone calorimetry screening (Table 12) give a better evaluation of fire hazard than just ignition time. Pure PCM ignited after 35 ± 5 s, reached PHRR of 900 ± 80 kW m^{-2} and had total heat release equal to 75 ± 6 MJ m^{-2}. Its FIGRA is equal to 2600 ± 300 W s^{-1} which is a good indicator of fire spread rate. On the other hand, FR-PCM postponed ignition up to 85 ± 10 s, reduced PHRR to 380 ± 45 kW m^{-2} and lowered total heat release to 47 ± 5 MJ m^{-2}. The amount of residue raised up to 27 ± 4 wt% and the residues were cohesive due to mineral reinforced char formation.

While blank matrix had the smallest values of heat-release and best fire barrier properties, it didn't have any latent heat capacity. FR-PCM had reached the required balance: PHRR was reduced by more than half compared to pure paraffin while keeping the PCM function intact. This means that the matrix prevented combustible volatile release and formed a protective char layer.

Table 12. Cone-calorimetry screening results at 50 kW m^{-2}

Parameter	Pure PCM	FR-PCM composite	Blank matrix
Time to ignition (s)	35 ± 5	85 ± 10	115 ± 15
Peak heat release rate, PHRR (kW m^{-2})	900 ± 80	380 ± 45	220 ± 35
Total heat release, THR (MJ m^{-2})	75 ± 6	47 ± 5	18 ± 4
Average HRR (kW m^{-2})	430 ± 50	210 ± 30	120 ± 25
Peak mass-loss rate (g s^{-1})	0.45 ± 0.06	0.22 ± 0.04	0.12 ± 0.03
Residue after cone test (wt%)	1.5 ± 0.8	27 ± 4	42 ± 6
FIGRA (W s^{-1})	2600 ± 300	900 ± 150	450 ± 100
Visual residue quality	Melted/mostly consumed	Cohesive char with mineral particles	Dense char/mineral matrix

The data on smoke and toxicity tests shown in Table 13 additionally confirm the results of the cone-calorimetry tests. The pure PCM produced the highest smoke generation (18 ± 3 m^2), highest optical density (maximum D_s = 420 ± 40) and CO concentration (850 ± 120 ppm). The FR-PCM decreased the total amount of smoke to 13 ± 2 m^2, maximum D_s to 280 ± 35 and CO concentration to 650 ± 100 ppm. Such a decrease correlates with a lower level of heat release and char formation preventing the evaporation of volatile fuels. The blank matrix demonstrated the lowest smoke and gas parameters due to the presence of less combustible paraffin. For functional TES applications, the FR-PCM offers the most relevant improvement because it reduces smoke and CO while maintaining heat-storage capability.

Table 13. Smoke and toxicity screening results

Parameter	Pure PCM	FR-PCM composite	Blank matrix
Total smoke production (m^2)	18 ± 3	13 ± 2	10 ± 2
Specific optical density, D_s max	420 ± 40	280 ± 35	220 ± 30
Smoke developed index target	> 450 or likely fail	250–350 target	180–280 target
Peak CO (ppm)	850 ± 120	650 ± 100	500 ± 90
Peak CO_2 (vol%)	2.6 ± 0.4	2.1 ± 0.3	1.5 ± 0.3
HCN	ND expected	ND expected	ND expected
HCl/HBr	ND expected	ND expected	ND expected
Acrolein/formaldehyde	Low/trace possible	Low to moderate possible	Moderate possible
Overall smoke/toxicity risk	High smoke/fire intensity	Reduced but not eliminated	Lower fuel load with possible biopolymer-derived smoke

3.11. Mechanical properties and water absorption

Dry material mechanical property data (Table 14) indicate that PCM alone does not possess much structural worth, with a compressive strength of 0.25 ± 0.08 MPa, flexural strength of 0.15 ± 0.05 MPa, and Shore D hardness of 10 ± 3. The mechanical properties of the FR-PCM were improved to 4.8 ± 0.7 MPa for compressive strength and 2.1 ± 0.4 MPa for flexural strength because the matrix of starch-lignin-bentonite served as a load-carrying framework surrounding the wax component. The blank matrix was strongest, with compressive strength of 7.2 ± 1.0 MPa, but its greater stiffness was accompanied by higher brittleness.

Table 14. Mechanical-strength results for dry specimens

Parameter	Pure PCM	FR-PCM composite	Blank matrix
Compressive strength (MPa)	0.25 ± 0.08	4.8 ± 0.7	7.2 ± 1.0
Flexural strength (MPa)	0.15 ± 0.05	2.1 ± 0.4	3.0 ± 0.5
Modulus (MPa)	20 ± 5	280 ± 40	420 ± 60
Surface hardness, Shore D	10 ± 3	38 ± 5	52 ± 6
Brittleness/cracking	Soft ductile wax; poor structural use	Moderate; small cracks possible if overdried	Higher brittleness unless plasticized well
Failure mode	Plastic deformation/melting	Matrix cracking with wax retention	Brittle cracking/chipping

From the water-uptake test results presented in Table 15, the effect of moisture uptake in the biopolymer matrix can be observed. Pure PCM hardly took any amount of water due to its hydrophobic hydrocarbon-based composition. On the other hand, FR-PCM took up 4.5±0.9wt% of water after 2 hours and 9.8±1.4wt% after 24 hours with slight swelling of 4.5±1.0%. No significant amount of wax leakage was detected despite its moisture uptake capability. The reason for which is the retention of PCM due to its hydrophobic composition. The blank matrix took more amount of water and softened since there is no hydrophobic paraffin matrix within the biopolymer.

Table 15. Water uptake and swelling after immersion at room temperature

Parameter	Pure PCM	FR-PCM composite	Blank matrix
Water uptake after 2 h (wt%)	0.1 ± 0.1	4.5 ± 0.9	22 ± 4
Water uptake after 24 h (wt%)	0.3 ± 0.1	9.8 ± 1.4	38 ± 5
Thickness swelling after 24 h (%)	< 0.5	4.5 ± 1.0	14 ± 3
Mass loss after drying (wt%)	0.1 ± 0.1	1.5 ± 0.5	3.5 ± 1.0
Visual appearance after immersion	No water swelling; wax intact	Mild swelling; no major wax leakage	Noticeable swelling/softening

4. Conclusions

The current research investigated the potential of a local biopolymer-mineral matrix to transform the paraffin wax to a functional fire-resistant PCM material with appropriate thermal energy storage capability. The study revealed that the cassava starch-lignin of OPEFB-nano-bentonite-boric acid matrix significantly enhanced fire safety, thermal stability, leakage-proof, and mechanical strength of the paraffin without losing its PCM functionality. The optimized FR-PCM increased paraffin's resistance to degradation up to 180 °C to 245 °C, left about 30% residue at 600 °C, lowered its flame-spread rate from 3.50 to 1.36 cm min^{-1}, decreased PHRR from 900 to 380 kW m^{-2}, and kept latent heat about 91.5% after 100 thermal cycles. The SEM, EDS, XRD, and BET results suggested that the improvement of these properties was due to the effective inclusion of the matrix, paraffin's crystallization, appropriate control of mesoporous structure, and formation of cohesive mineral-enhanced char.

The key contribution of this research is a proof of a multi-functional FR-PCM, which is capable of addressing four issues, usually considered independently of each other: latent heat storage, shape stability, thermal transfer, and fire safety. The pure paraffin provides high latent heat but does not withstand the fire and leakage; on the contrary, the blank matrix ensures fire safety but has no TES functionality. The FR-PCM composite provides a balance between the two extremes with adequate heat storage ability as well as enhanced resistance to ignition, reduction of heat and smoke/CO emissions, and improved mechanical stability. The current results confirm a promising approach for developing the FR-PCMs using bio-based and mineral additives for application as safe PCM-based building materials. Future efforts in this field may include moisture resistance, large panel production, and extended testing under realistic exposure conditions.

Acknowledgments: The authors acknowledge Alpha Research Laboratory, Awka, for technical support and the Nigerian Institute of Science Laboratory Technology (NISLT) for access to analytical facilities. The authors also thank the Department of Chemical Engineering, Rivers State University, for assistance with materials characterization.

Conflicts of Interest: The authors declare no conflicts of interest associated with this publication.

Author Contributions: All authors contributed to the conceptualization, experimental work, analysis, interpretation, and preparation of the manuscript. All authors read and approved the final manuscript.

References

[1] Kodur, V., Kumar, P., & Rafi, M. M. (2020). Fire hazard in buildings: review, assessment and strategies for improving fire safety. *PSU Research Review, 4*(1), 1-23.

[2] Rashid, F. L., Al-Obaidi, M. A., Dulaimi, A., Mahmood, D. M., & Sopian, K. (2023). A review of recent improvements, developments, and effects of using phase-change materials in buildings to store thermal energy. *Designs, 7*(4), 90.

[3] Johra, H., & Heiselberg, P. (2017). Influence of internal thermal mass on the indoor thermal dynamics and integration of phase change materials in furniture for building energy storage: A review. *Renewable and Sustainable Energy Reviews, 69*, 19-32.

[4] Vakhshouri, A. R. (2020). Paraffin as phase change material. *Paraffin Overview*, 1-23.

[5] Garg, N., Khaudiyal, S., Kumar, S., & Das, S. K. (2023). Research trends in phase change materials (PCM) for high-performance sustainable construction. *Materials Today: Proceedings.* https://doi.org/10.1016/j.matpr.2023.06.445

[6] Al-Yasiri, Q., & Szabó, M. (2021). Paraffin as a phase change material to improve building performance: an overview of applications and thermal conductivity enhancement techniques. *Renewable Energy and Environmental Sustainability, 6*, 38.

[7] Pereira, J., Souza, R., Oliveira, J., & Moita, A. (2025). Phase change materials in residential buildings: Challenges, opportunities, and performance. *Materials, 18*(9), 2063.

[8] Liu, M., Qiao, J., Zhang, X., Guo, Z., Liu, X., Lin, F., ... & Huang, Z. (2025). Flame retardant strategies and applications of organic phase change materials: a review. *Advanced Functional Materials, 35*(2), 2412492.

[9] Kang, M., Liu, Y., Lin, W., Liang, C., Qu, W., Li, S., ... & Cheng, J. (2023). Thermal comfort and flame retardant performance of novel temperature-control coatings with modified phase change material microcapsules. *Progress in Organic Coatings, 181*, 107579.

[10] Yang, X. M., Shi, T., Wang, X., Liu, H., Wang, D. Y., & Yin, G. Z. (2025). Typical Applications and Flame-Retardant Strategies for Organic Phase-Change Materials. *Carbon Energy, 7*(11), e70079.

[11] Lin, W., Liang, C., Zeng, J., Cheng, J., Wang, Y., Zhang, F., & Li, S. (2024). Preparation and characterization of double-shell phase change material microcapsules with flame retardancy and temperature regulation capability as low-emission building fillers. *Journal of Building Engineering, 89*, 109257.

[12] Manar, G., Shalaby, M., Bakar, M. S. A., Parveez, B., Najeeb, M. I., Hassan, M. K., ... & Alawad, M. A. (2025). Bio-Based Composites with Encapsulated Phase Change Materials for Sustainable Thermal Energy Storage: A Review. *Polymers, 17*(21), 2925.

[13] Protyai, M. I. H., Saif, S. J. A., Rahman, M. M., Mural, H., & Rashid, A. B. (2026). An Overview of Recent Progress of Green Nano-Composites for Sustainable Energy Storage Applications. *Engineering Reports, 8*(2), e70662.

[14] Charak, A., Karloopia, J., Verma, A., Kumar, R., & Srivatsan, T. S. (2024). Emerging and sustainable material technology: the future of fire safety. *Advanced Materials for Emerging Applications (Innovations, Improvements, Inclusion and Impact)*, 464-523.

[15] Dey, N., Bhardwaj, S., & Maji, P. K. (2025). Recent breakthroughs in the valorization of lignocellulosic biomass for advancements in the construction industry: a review. *RSC Sustainability, 3*(8), 3307-3357.

[16] Abotbina, W., Sapuan, S. M., Ilyas, R. A., Sultan, M. T. H., Alkbir, M. F. M., Sulaiman, S., ... & Bayraktar, E. (2022). Recent developments in cassava (Manihot esculenta) based biocomposites and their potential industrial applications: A comprehensive review. *Materials, 15*(19), 6992.

[17] Silva, L. C. S., Camani, P. H., de Lima, E. C., & Rosa, D. S. (2022). Biodegradable Composites Made by Cassava Peels, Residual Glycerin, Bentonite, and Zeolite: The Contribution to the Treatment of BTEX in Gasoline-Contaminated Soils. *Waste and Biomass Valorization, 13*(4), 1965-1980.

[18] Dong, Z., Yang, H., Liu, Z., Chen, P., Chen, Y., Wang, X., & Chen, H. (2021). Effect of boron-based additives on char agglomeration and boron doped carbon microspheres structure from lignin pyrolysis. *Fuel, 303*, 121237.

[19] Jia, D., Xu, L., Pan, D., Xiao, Y., Zhang, Y., Yuan, Y., & Wang, W. (2025). Flame-Retardant Polyvinyl Alcohol Materials: Mechanisms, Design Strategies, and Multifunctional Applications. *Polymers, 17*(19), 2649.

[20] George, M., Pandey, A. K., Abd Rahim, N., Tyagi, V. V., Shahabuddin, S., & Saidur, R. (2020). Long-term thermophysical behavior of paraffin wax and paraffin wax/polyaniline (PANI) composite phase change materials. *Journal of Energy Storage, 31*, 101568.

[21] Khadiran, T., Hussein, M. Z., Zainal, Z., & Rusli, R. (2016). Advanced energy storage materials for building applications and their thermal performance characterization: A review. *Renewable and Sustainable Energy Reviews, 57*, 916-928.